



Effect of Solvent on Third-Order Nonlinear Optical Behavior of Reactive Blue 19 Dye

S. Jeyaram¹ · J. Naseer² · S. Punitha³

Received: 18 July 2021 / Accepted: 27 August 2021 / Published online: 17 September 2021

© The Author(s), under exclusive licence to Springer Science+Business Media, LLC, part of Springer Nature 2021

Abstract

The present work focuses the study of effect of solvent on third-order nonlinear optical (NLO) properties of reactive blue 19 dye dissolved in various polar solvents, namely ethanol, DMF and DMSO, respectively. Fourier Transform Infrared Spectroscopy (FT-IR) was used to find the functional groups present in reactive blue 19 dye. Third-order NLO features of reactive blue 19 dye was examined by a low power continuous wave laser of 650 nm wavelength. Reactive blue 19 dye exhibit negative nonlinear index of refraction of the power of 10^{-7} cm²/W and the nonlinear coefficient of absorption of the order of 10^{-3} cm/W. Both positive and negative nonlinear absorption coefficient of reactive blue 19 dye in different polar solvents is due to the characteristic behavior of saturable and reverse saturable absorption. Third-order NLO susceptibility of reactive blue 19 dye in polar solvents was determined to be the power of 10^{-6} esu. The experimental results reveal that the dye sample reactive blue 19 is a potential material for nonlinear optical applications.

Keywords Polar solvents · FT-IR · Z-scan · NLO susceptibility

Introduction

Novel NLO materials have attracted widespread attention over the decades due to their potential applications in high harmonic generation in laser, optoelectronic oscillators, optical switching, three-dimensional optical data storage, ultrafast photonics stability, optical computing and optical power limiting [1–3]. A wide variety of materials are known to be optically nonlinear under continuous and pulsed wave laser excitation [4–7]. Of the various materials, organic materials have gained significance attention because of their large third-order nonlinearity, good processability, ultrafast response time, greater flexibility in terms of molecular

structure and higher optical damage threshold [8–10]. In particular, conjugated organic dyes have attracted more consideration because of their strong π -electron delocalization with donor and acceptor electrons. This causes higher molecular polarizability and thus results in a larger third-order nonlinear optical susceptibility [11]. The polarization of the dye molecules is originating from the main chain of delocalization of π -conjugated system. The large π -electron delocalization of the compound has good mechanical, electrochemical, photochemical and processing properties [12, 13]. In order to obtain a large value of third-order NLO susceptibility and second-order polarizability, the molecules should be a large polarization, large absorption wavelength, large dipole moment and a small value of energy gap [14]. The π -conjugated dyes are attained the above characteristics and therefore organic dyes may preferably be a good third-order NLO materials. Azo, Indigo, Anthraquinone, Triphenylmethane, Triarylmethane, etc., are the major chromophores found in commercial dyes. Reactive blue 19 dye is a family of anthraquinone, which appears dark blue powder and highly soluble in polar solvents.

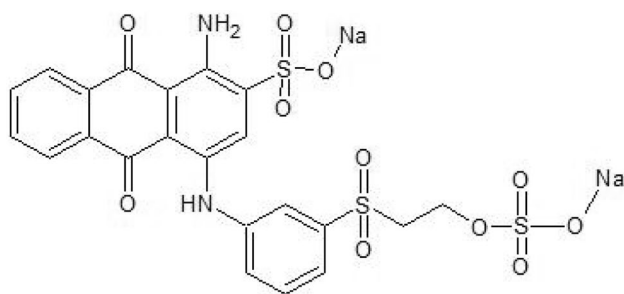
Molecular surrounding environment has had an influence on the physical and chemical behavior of organic materials [15, 16]. The interaction between solute and solvent is divided into specific (hydrogen bonding) and non-specific

✉ S. Jeyaram
jeyaram.msc@gmail.com

¹ Department of Physics, School of Engineering and Technology, Surya Group of Institutions, Vikravandi, Villupuram, Tamilnadu 605652, India

² Department of Physics, St. Michael College of Engineering and Technology, Kalayarkoil, Sivaganga, Tamilnadu 630551, India

³ Department of Electrical and Electronics Engineering, Sri Manakula Vinayagar Engineering College, Madagadipet, Puducherry 605107, India



Molecular Formula: $C_{22}H_{16}N_2Na_2O_{11}S_3$

Fig. 1 Molecular structure of reactive blue 19 dye

(dielectric enhancement) interactions and the effect of solvent on solute molecules can be determined by using solvatochromism and solvent polarity index [17]. Z-scan technique [18, 19] is a single beam technique that concurrently evaluates the real and imaginary components of the third-order NLO susceptibility, as well as the sign and magnitude of nonlinear index of refraction and nonlinear coefficient of absorption of the sample can be obtained from simple experimental calculations. Third-order NLO susceptibility ($\chi^{(3)}$) of the sample is determined from real and imaginary factors of the third-order NLO susceptibility. The real part of the third-order NLO susceptibility is directly proportional to nonlinear refractive index, while the imaginary part of the third-order NLO susceptibility is directly related to nonlinear coefficient of absorption. Therefore, n_2 and β are the essential parameters to calculate the third-order NLO susceptibility, which is determined from closed and open aperture Z-scan technique. A circular aperture is employed in closed aperture technique and placed at far-field with a linear aperture transmittance of $S=0.40$. The aperture was replaced with a convex lens to collect the total transmittance of the sample is known as open aperture ($S=1$) technique. This paper reports the third-order NLO susceptibility of reactive blue 19 dye dissolved in different polar solvents such as ethanol, DMF and DMSO using a continuous wave laser working at 650 nm wavelength.

Table 1 Linear and spectral parameters of polar solvents

Solvent	Linear refractive index (n_0)	Dielectric constant (ϵ)	Hydrogen bond donor (α)	Hydrogen bond acceptor (β)	Polarizability (π^*)	Linear absorption coefficient (α_0/cm)
Ethanol	1.361	24.50	0.86	0.75	0.52	7.07
DMSO	1.479	46.68	0.00	0.76	1.00	7.48
DMF	1.430	38.00	0.00	0.69	0.88	4.90

Experimental

Sample

Sigma Aldrich provided the polar solvents and reactive blue 19 dye. The stock solution of 0.05 mM concentration was prepared by dissolving reactive blue 19 dye into different polar solvents of ethanol, DMF and DMSO, respectively. Figure 1 represents the chemical structure of reactive blue 19 dye.

Method

The UV–Vis absorption spectrum of reactive blue 19 dye was determined using UV 1601 Shimadzu spectrometer. The spectral characteristics and linear absorption coefficient of polar solvents is tabulated in Table 1. The Perkin Elmer spectrometer was used to find the chemical composition of the sample.

Z-scan technique was highly preferred by the researchers due to simplicity, accuracy, efficient and highly sensitive to measure the nonlinear index of refraction, n_2 and nonlinear coefficient of absorption, β . Figure 3 depicts the schematic of Z-scan technique. A single beam Z-scan technique consists of a solid state diode laser operating at 650 nm wavelength with 5 mW power. The beam was focused by a convex lens with focal length of 50 mm. A cuvette with path length of 1 mm was used and moved between $-Z$ and $+Z$ positions using a micrometer translational stage. The transmittance of the sample was measured by a power meter at far-field. The thin sample approximation was validated in the present study, because the measured Rayleigh length is greater than sample length.

Theory

The phase modulation of the beam is transferred to amplitude modulation when the nonlinear medium is moved through the focal plane of a positive lens is the principle of Z-scan method. Two distinct methods such as closed and open aperture methods were commonly applied in Z-scan technique to measure the nonlinear index of refraction, n_2

Fig. 2 UV–Vis absorption spectrum of reactive blue 19 dye

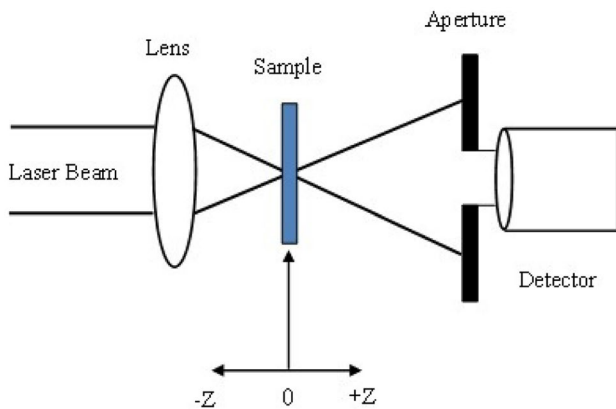
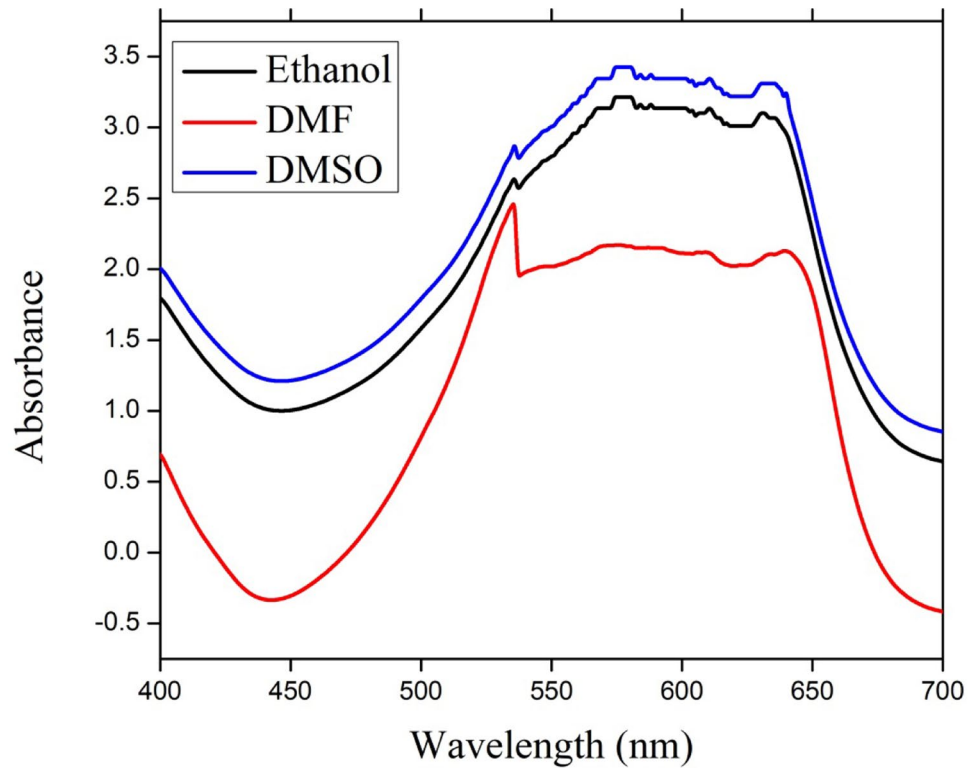


Fig. 3 Experimental Z-scan technique

and nonlinear coefficient of absorption, β . The nonlinear index of refraction of the sample was calculated from the following equations derived from Ref. [18]:

The transmittance of the sample is proportional to the on-axis phase shift $\Delta\Phi_0$ which is calculated from the fitting curve of closed aperture using the relation,

$$T(z) = 1 - \Delta\theta_o \frac{4X}{(X^2 + 1)(X^2 + 9)} \tag{1}$$

where $X = Z/Z_0$.

$$\Delta\theta_0 = \frac{\Delta T_{p-v}}{0.406(1 - S)^{0.25}}$$

where ΔT_{p-v} = Difference between normalized transmittance peak and normalized transmittance valley. S = Linear aperture transmittance is given by

$$S = \frac{[1 - \exp(-\alpha_0 L)]}{\alpha_0}$$

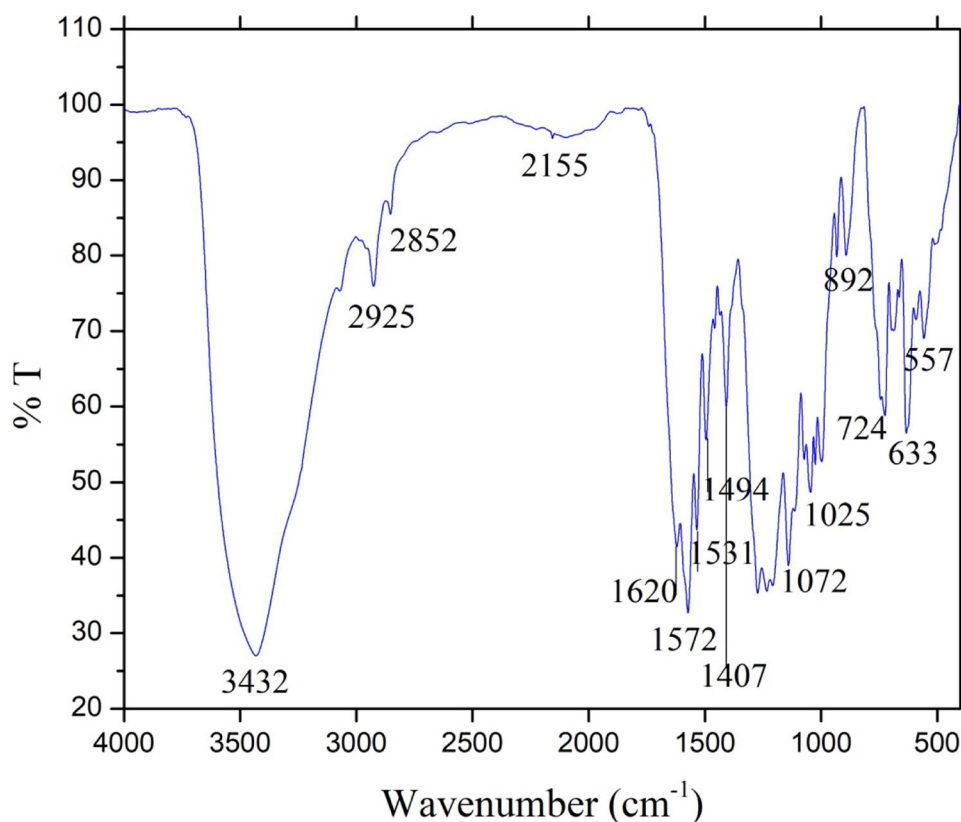
where α_0 = Linear absorption coefficient; L = Length of the sample (1 mm); The n_2 of the sample is determined by using the relation,

$$n_2 = \frac{\Delta\theta_0 \lambda}{2\pi I_0 L_{eff}} \left(\frac{\text{cm}^2}{W} \right) \tag{2}$$

where I_0 = Intensity of the beam; L_{eff} = Effective thickness of the sample; λ = Wavelength of the laser beam.

On the other hand, the transmittance of the sample from nonlinear coefficient of absorption is given by,

$$T(z, s = 1) = \sum_{m=0}^{\infty} \frac{[-q_o(z)]^m}{(m + 1)^{3/2}} q_o(0) < 1 \tag{3}$$

Fig. 4 FT-IR spectrum of reactive blue 19 dye**Table 2** Molecular vibration of Reactive blue 19 dye

Wavenumber (cm ⁻¹)	Group
724	C–H bending
892	C–H bending
1025	C–O stretching
1072	S=O stretching
1407	O–H bending
1494	C–H bending
1531	C=C stretching
1572	C=C stretching
1620	C=C stretching
2852	C–H stretching
2925	C–H stretching
3432	O–H stretching

The nonlinear absorption coefficient of the sample is defined as:

$$\beta = \frac{2\sqrt{2}\Delta T}{I_0 L_{eff}} \left(\frac{\text{cm}}{\text{W}} \right) \quad (5)$$

The real and imaginary factors of third-order optical nonlinearity is directly proportional to nonlinear index of refraction and nonlinear coefficient of absorption is given by,

$$\text{Re}[\chi^{(3)}](esu) = 10^4 \frac{\epsilon_0 c^2 n_0^2}{\pi} n_2 \left(\frac{\text{cm}^2}{\text{W}} \right) \quad (6)$$

$$\text{Im}[\chi^{(3)}](esu) = 10^2 \frac{\epsilon_0 c^2 n_0^2 \lambda}{4\pi^2} \beta \left(\frac{\text{cm}}{\text{W}} \right) \quad (7)$$

where ϵ_0 = vacuum permittivity; c = light velocity in vacuum.

The absolute value of third-order optical nonlinearity $\chi^{(3)}$ for the sample is calculated using the equation,

$$\chi^{(3)}(esu) = \left[(\text{Re}(\chi^{(3)}))^2 + (\text{Im}(\chi^{(3)}))^2 \right]^{\frac{1}{2}} \quad (8)$$

$$q_0(z) = \frac{\beta I_0 L_{eff}}{(1 + Z^2/Z_0^2)} \quad (4)$$

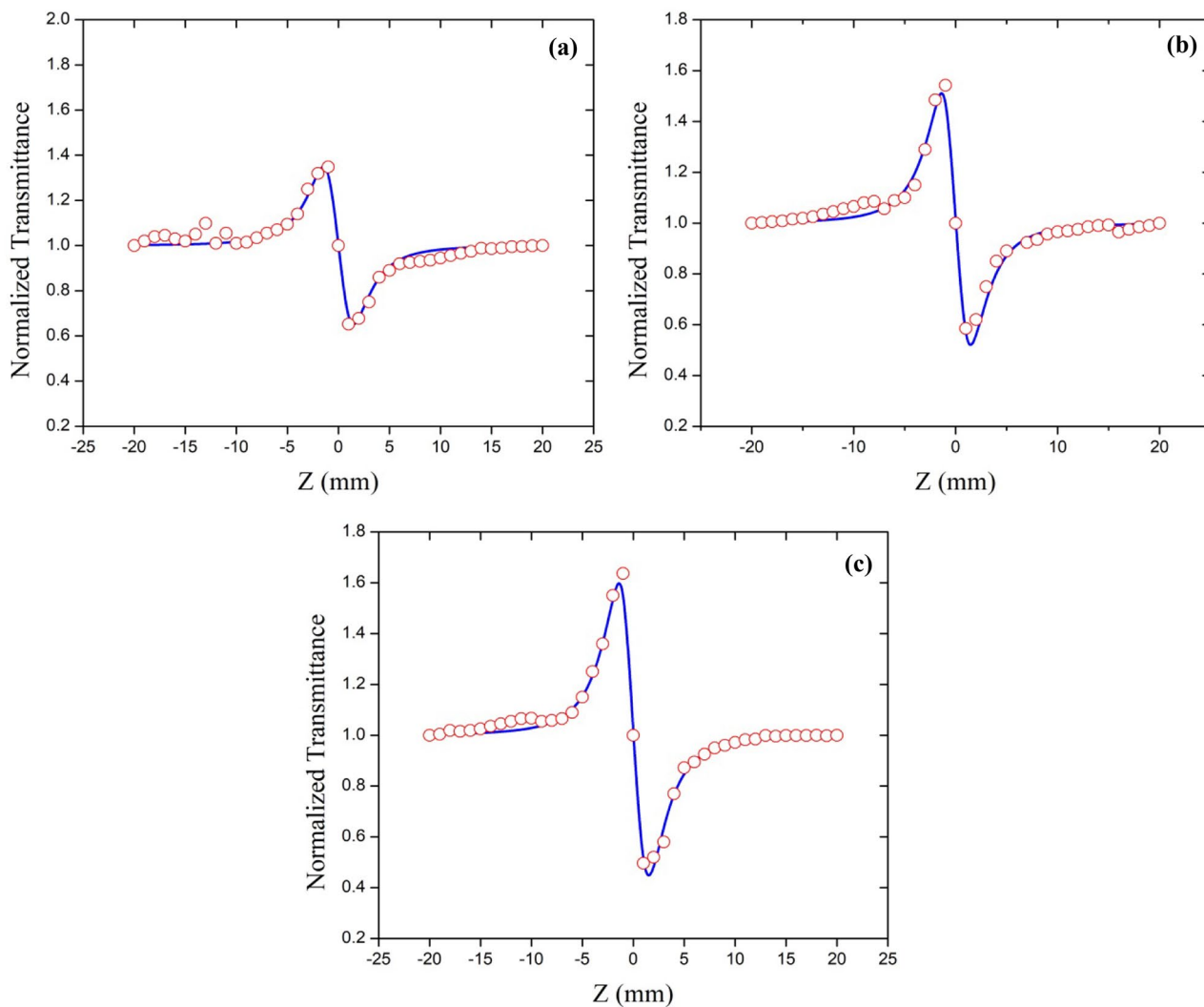


Fig. 5 NLR curve of reactive blue 19 dye in (a) Ethanol, (b) DMF, (c) DMSO

Table 3 Measured third-order NLO characteristics of Reactive blue 19 dye in polar solvents

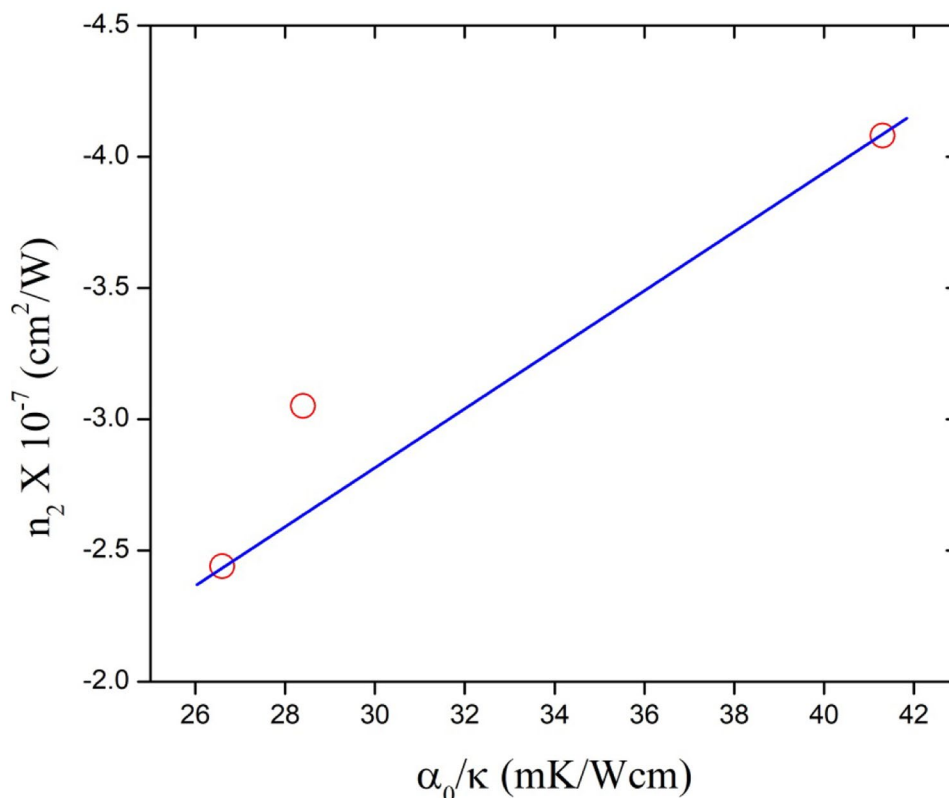
Solvent	$n_2 \times 10^{-7}$ (cm ² /W)	$\beta \times 10^{-3}$ (cm/W)	Re ($\chi^{(3)}$) $\times 10^{-6}$ (esu)	Im ($\chi^{(3)}$) $\times 10^{-7}$ (esu)	$\chi^{(3)}$ $\times 10^{-6}$ (esu)	$dn/dT \times 10^{-4} \text{ K}^{-1}$
Ethanol	-2.44	-9.65	-0.92	-1.65	0.94	-0.95
DMF	-3.05	5.11	-1.14	0.96	1.14	-1.84
DMSO	-4.08	7.17	-1.63	1.45	1.64	-2.31

Results and discussion

The UV–Visible absorption spectrum of reactive blue 19 dye in polar solvents is depicted in Fig. 2. Different peaks have been observed in the visible region and the predominant peak is 638 nm which is the resonant absorption range of used laser source. The longer wavelength in the UV–Visible

spectrum is owing to high conjugated π -electrons in reactive blue 19 dye. Furthermore, the observed peaks in the UV–Visible region may be due to amine group in 1, 4 positions in the dye sample. This group is responsible for bathochromic shift in reactive blue 19 dye [19]. Bathochromic shift in reactive blue 19 dye is owing to charge transfer between amino group and oxygen atom of carbonyl group .

Fig. 6 Variation of NLR as a function of α_0/κ in different polar solvents



FT-IR analysis of reactive blue 19 dye in the range between 500 and 4000 cm^{-1} is shown in Fig. 4. The specific vibrations were mentioned in FT-IR spectrum is based on the standard IR spectrum table and Sigma Aldrich charts. The summary of molecular vibration of reactive blue 19 dye is presented in Table 2. An intense vibration peak at 3452 cm^{-1} is due to stretching vibration of hydroxyl group. The C–H stretching groups are respectively existed at 2925 cm^{-1} and 2852 cm^{-1} . Furthermore, the weak bands at 1620 cm^{-1} , 1572 cm^{-1} and 1531 cm^{-1} are corresponds to aromatic stretching of C=C group. The stretching of aromatic compounds C=C gives rise in intermolecular charge transfer (ICT) between donor and acceptor electrons which in turn increase the NLO responses in reactive blue 19 dye. The medium band at 1494 cm^{-1} and 1407 cm^{-1} are owing to bending of –CH and –OH group. The vibration at 1072 cm^{-1} is due to S=O stretching, the sulfonate group is connected to benzene ring. The weak band at 1025 cm^{-1} is due to stretching of –CO group. The vibrations at 894 cm^{-1} and 724 cm^{-1} are owing to C–H aliphatic bending frequency of reactive blue 19 dye.

Figure 5 (a–c) illustrates the closed-aperture NLR curve of reactive blue 19 dye in different polar solvents of ethanol, DMF and DMSO. The NLR measurements using closed aperture Z-scan technique is sensitive to both NLR and NLA. Therefore, the estimation of pure NLR is carried out

by dividing closed aperture data by the corresponding open aperture data. The NLR curve of the dye sample in polar solvents exhibits a peak-valley transmittance is the result of self-defocusing. The defocusing effect in reactive blue 19 dye is owing to thermal effect. Thermal effect is the phenomenon caused by the localized absorption of the propagating continuous wave laser and thus creating the spatial temperature profile nonlocally across it. Under continuous wave laser radiation, the contribution of thermal effects is dominant and neither be avoided nor ignored. The thermal nonlinearity and the third-order process were confirmed by the separation between peak and valley transmittance. If the separation is greater than 1.7 times Z_R is the clear sign of thermal nonlinearity [20]. In present work, the NLR curve of reactive blue 19 dye in polar solvents exhibits the peak-valley separation of $2Z_R$. The nonlinear index of refraction of reactive blue 19 dye in polar solvents is calculated by using Eq. (2) and the value is tabulated in Table 3. From Table 3, the value of n_2 of reactive blue 19 dye in DMSO is higher than that of other polar solvents such as DMF and ethanol. This may be due to the fact that, the high polar solvent (DMSO) interacts with solute molecules gives rise in nonlinear index of refraction. Under 650 nm continuous wave irradiation, the nonlinearity of the sample is owing to thermal origin and the thermo-optic coefficient as a function of nonlinear index of refraction is given by

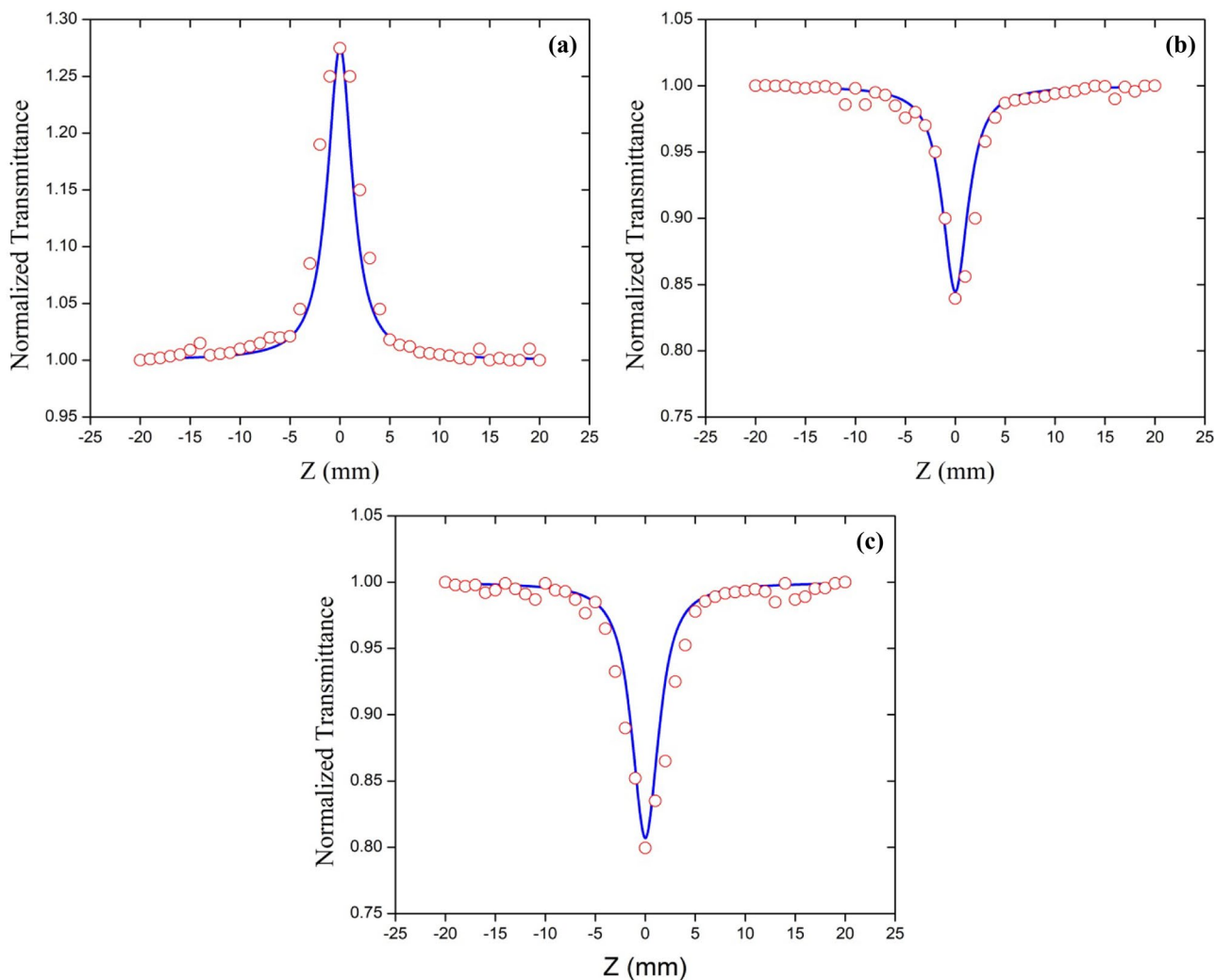


Fig. 7 NLA curve of reactive blue 19 dye in (a) Ethanol, (b) DMF, (c) DMSO

Table 4 Third-order NLO susceptibility of some reported anthraquinone dyes

S. no	Name of the dye	λ (nm)	Method	$\chi^{(3)}$ (esu)	References
1	1,5 diaminoanthraquinone (Acetone)	532	Z-scan	7.26×10^{-12}	[2]
2	Reactive blue 4	635	Z-scan	1.86×10^{-6}	[3]
3	Acid green 25	635	Z-scan	3.11×10^{-7}	[11]
4	1,4-diamino-2,3-diphenoxy Anthraquinone	532	Degenerate four-wave mixing	1.16×10^{-12}	[21]
5	Disperse blue 14	635	Z-scan	1.33×10^{-7}	[22]

$$n_2 = \frac{dn}{dT} \frac{\alpha_0 \omega_0^2}{4k} \tag{9}$$

where α_0 is the linear absorption coefficient, k is the thermal conductivity of the solvents and ω_0 is the beam waist at the focal point, respectively. Therefore, the linear absorption coefficient and thermal conductivity of polar solvents play important role and highly depends on nonlinear index of refraction. It is observed from Fig. 6, the third-order nonlinear index of refraction, n_2 is increases with increase the value of (α_0/k) . The thermo-optic coefficient of reactive blue 19 dye in different polar solvents is tabulated in Table 3.

Figure 7 (a–c) shows the nonlinear absorption curve of reactive blue 19 dye in polar solvents. The negative and positive nonlinear absorption mechanism was observed in the dye sample is due to saturable and reverse saturable absorption nonlinearity. A switch over from saturable absorption to reverse saturable absorption (RSA) in reactive blue 19 dye

Fig. 8 NLR as a function of (a) HBA, (b) HBD and (c) polarizability

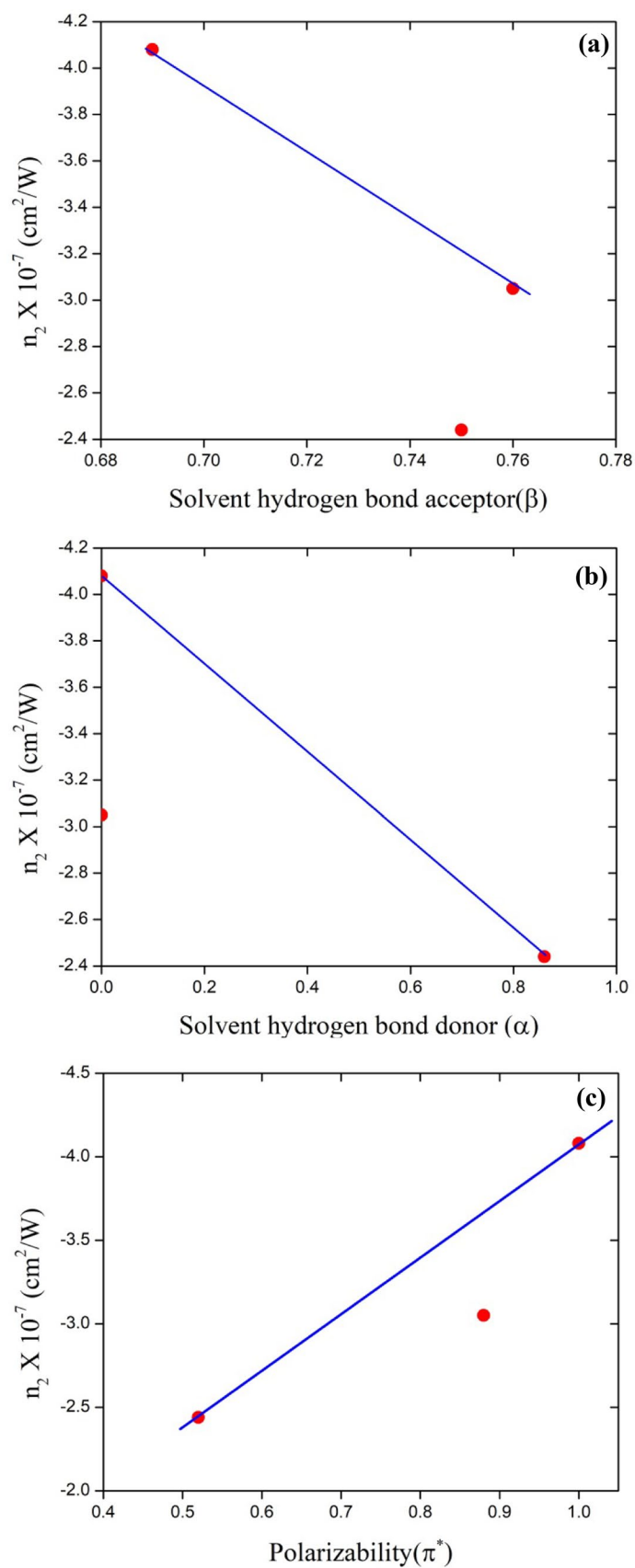


Fig. 9 NLA as a function of (a) HBA, (b) HBD and (c) polarizability

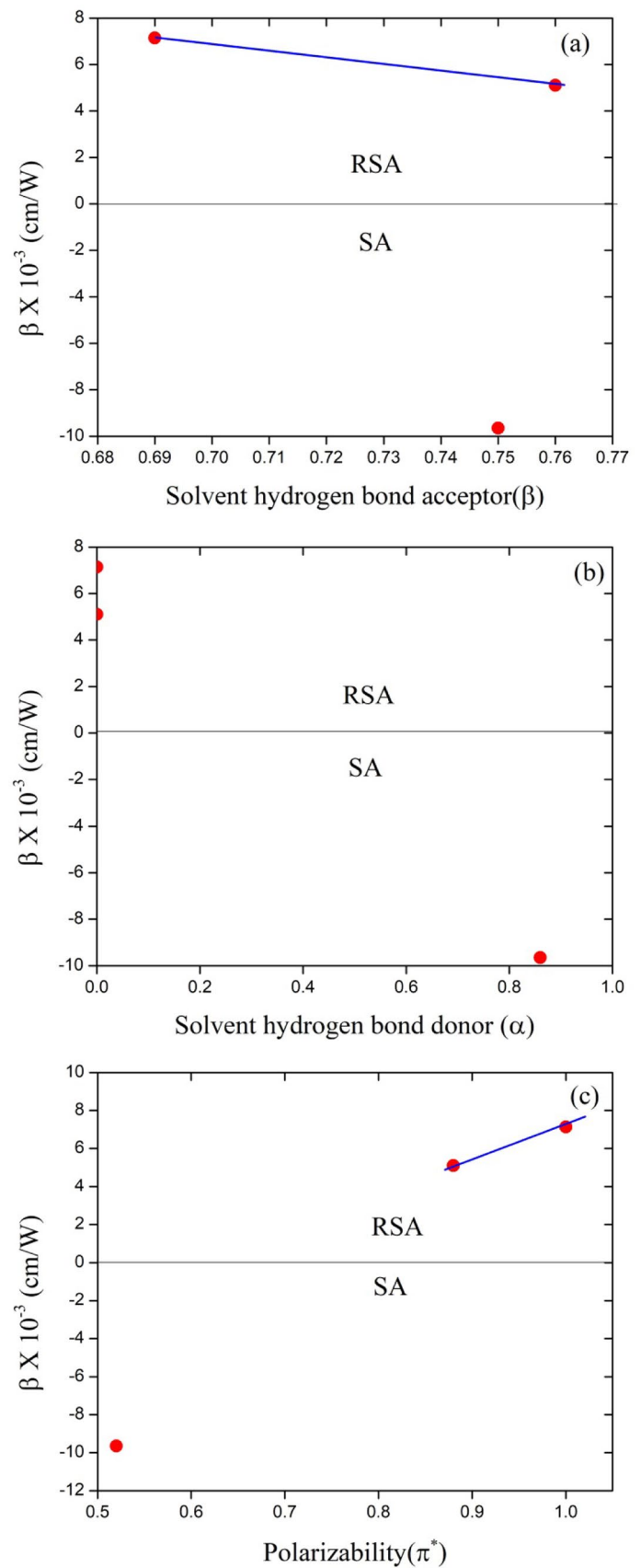
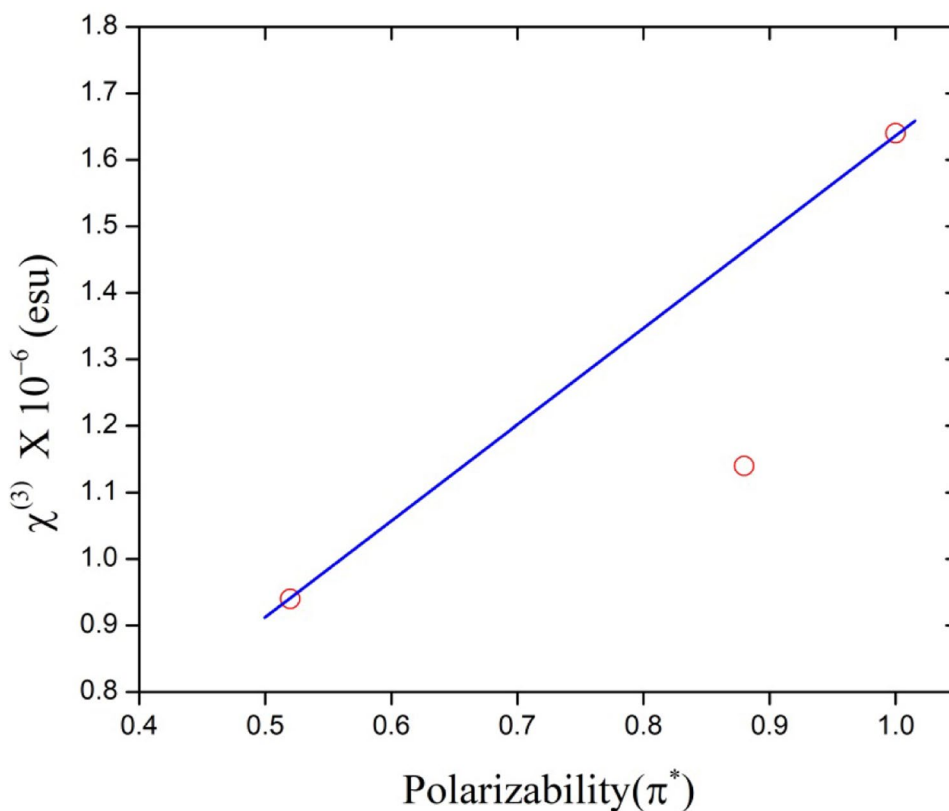


Fig. 10 Polarizability Vs Third-order NLO susceptibility



may be due to increase in solvent polarizability of the polar solvents. The nonlinear absorption mechanism of both saturable and reverse saturable absorption can be approximately explained by a five-level model [3]. Generally, a transition was caused between ground state and an excited state is due to interaction of high intense laser beam with molecules in the ground state. The transition between first singlet state (S_1) and first triplet state (T_1) via intersystem crossing is known as saturable absorption. Under this condition, RSA takes place if the absorption is stronger between first singlet states (S_1) and excited singlet state (S_2) or first triplet state (T_1) and excited triplet state (T_2). The saturable and reverse saturable absorption characteristics of the dye sample are depends on the life time of ground and excited state and solute–solvent interaction. The nonlinear coefficient of absorption of reactive blue 19 dye in polar solvents is calculated by using Eq. (5) and the values are presented in Table 3. Third-order nonlinear susceptibility of reactive blue in polar solvents is calculated using the Eq. (8) and the measured value is tabulated in Table 3. From Table 3, the reactive blue 19 dye in DMSO exhibits a large value of third-order susceptibility than that of other polar solvents such as ethanol

and DMF. This may be due to large value of polarizability of the solvents and high polar solvents gives large value of $\chi^{(3)}$. For the interest of researchers, the observed results are compared with some reported anthraquinone dyes, which are presented in Table 4. The obtained results are larger than that of reported dyes [2, 3, 11, 21, 22].

Third-order NLO parameters of the dye sample are depends on various spectral characteristics of solvents such as solvent hydrogen bond donor, solvent hydrogen bond acceptor and solvent polarizability, respectively. In order to determine the effect of solvent polarity parameters on nonlinear optical parameters, the value of third-order nonlinear parameters was plotted as function solvent polarity parameters (Figs. 8, 9, 10). Figures 8 (a & b) and 9 (a & b) shows the nonlinear refraction (NLR) and nonlinear absorption (NLA) of reactive blue 19 dye in polar solvents as a function of solvent hydrogen bond acceptor (HBA) and solvent hydrogen bond donor (HBD). From Figs. 8 (a & b) and 9 (a & b), the values of NLR and NLA decrease with increase in HBA and HBD. Also it is observed from Figs. 8 (c) and 9 (c), the value of NLR and NLA of the dye sample increases with increase in solvent

polarizability. The value of third-order NLO susceptibility of reactive blue 19 dye in polar solvents are also increases with increase in polarity of the solvents (Fig. 10). Various parameters such as linear absorption, substituent and polarity of solvents are influenced in modifying the third-order NLO parameters of the dye sample. Based to the experimental results, the solvent polarizability is the profound effect on the third-order NLO parameters of the sample.

Conclusion

Third-order NLO behavior of reactive blue 19 dye in polar solvents was examined by a 5 mW power CW laser working at 650 nm wavelength. The linear and third-order NLO properties of dye sample were greatly dependent on solvent polarity. The closed aperture Z-scan traces of reactive blue 19 dye exhibits self-defocusing nonlinearity, while the open aperture Z-scan traces displays the behavior of both saturable and reverse saturable absorption. Transition from saturable absorption to reverse saturable absorption was observed due to increase in solvent polarity. The real and imaginary factors of the third-order NLO susceptibility of reactive blue 19 dye was measured to be the order of 10^{-6} esu and exhibit a large nonlinear optical susceptibility by dissolving the dye sample with high polar solvent (DMSO). The results are suggested that, the dye sample studied here is a potential candidate for applications in photonics and optoelectronics.

Author contribution Conceptualization—SJ; Methodology—JN and SJ; Validation—SP and SJ; Writing-review and editing—SP and SJ; Supervision—SJ.

Funding None.

Data availability The datasets generated during the current study is available from the corresponding author.

Code availability The software process in the current study is available from the corresponding author.

Declarations

Conflict of interest The authors declare that they have no conflict of interest.

References

- Kramer MA, Tompkin WR, Boyd RW (1986) Nonlinear optical interactions in fluorescein-doped boric acid glass. *Phys Rev A* 34: 2026–2031. <https://doi.org/10.1103/physreva.34.2026>
- Sreenath MC, Hubert Joe I, Rastogi VK (2018) Third-order optical nonlinearities of 1,-diaminoanthraquinone for optical limiting applications. *Opt Laser Technol* 108:218–234. <https://doi.org/10.1016/j.optlastec.2018.06.056>
- Jeyaram S, Hemalatha S, Geethakrishnan T (2020) Nonlinear refraction, absorption and optical limiting properties of disperse blue 14 dye. *Chem Phys Lett* 739:137037. <https://doi.org/10.1016/j.cplett.2019.137037>
- Zongo S, Sanusi K, Britton J, Mthunzi P, Nyokong T, Maaza M, Sahraoui B (2015) Nonlinear optical properties of natural laccase dye studied using Z-scan technique. *Opt Mater* 46:270–275. <https://doi.org/10.1016/j.optmat.2015.04.031>
- Jeyaram S (2021) Intermolecular charge transfer in donor-acceptor substituted triarylmethane dye for NLO and optical limiting applications. *J Mater Sci Mater Elect* 32:9368–9376. <https://doi.org/10.1007/s10854-021-05600-7>
- Ryasnyansky AI, Palpant B, Debrus S, Khalibullin R, Stepanov RL (2006) Nonlinear optical properties of copper nanoparticles synthesized in indium tin oxide matrix by ion implantation. *J Opt Soc Am B* 23:1348–1353. <https://doi.org/10.1364/JOSA.23.001348>
- Jeyaram S, Geethakrishnan T (2020) Spectral and third-order nonlinear optical characteristics of natural pigments extracted from coriandrum sativum. *Opt Mater* 107:110148. <https://doi.org/10.1016/j.optmat.2020.110148>
- He GS, Xu GS, Prasad PN, Reinhardt BA, Bhatt JC, Dillard AG (1995) Two-photon absorption and optical limiting properties of novel organic compounds. *Opt Lett* 20:435–437. <https://doi.org/10.1364/ol.20.000435>
- Bredas JL, Adant C, Tackx P, Persoons A, Pierce BM (1994) Third-order nonlinear optical response in organic materials: theoretical and experimental aspects. *Chem Rev* 94:243–278. <https://doi.org/10.1021/cr00025a0080>
- Davies RL, Samoc M (1997) Third-order nonlinear optical organic materials for photonic switching. *Curr Opin Solid State Mater Sci* 2:213–219. [https://doi.org/10.1016/S1359-0286\(97\)80068-X](https://doi.org/10.1016/S1359-0286(97)80068-X)
- Jeyaram S, Geethakrishnan T (2017) Third-order nonlinear optical properties of acid green 25 dye using Z-scan method. *Opt Laser Technol* 89:179–185. <https://doi.org/10.1016/j.optlastec.2016.10.006>
- Liu J, Gao B, Cheng Y, Xie Z, Geng Y, Wang L, Jing X, Wang F (2008) Novel white electroluminescent single polymer derived from fluorine and quinacridone. *Macromolecules* 41:1162–1167. <https://doi.org/10.1021/ma071235z>
- Pho TV, Zalar P, Garcia A, Nguyen TQ, Wudl F (2010) Electron injection barrier reduction for organic light-emitting devices by quinacridone derivatives. *Chem Commun* 46:8210–8212. <https://doi.org/10.1039/c0cc01596b>
- Jia J, Feng D, Sha Y, Zhou C, Liang G, She Y (2020) New quinacridone derivatives: synthesis, photophysical and third-order nonlinear optical properties. *Tetrahedron* 76:131057. <https://doi.org/10.1016/j.tet.2020.131057>
- Jeyaram S, Geethakrishnan T (2020) Solvent dependent linear and nonlinear optical characteristics of acid blue 3 dye. *J. Fluores* 30: 1161–1169. <https://doi.org/10.1007/s10895-020-02580-5>
- Khadem Sadigh M, Zakerhamidi MS (2017) Environmental effects on the nonlinear absorption properties of Methylene blue under different power of excitation beam. *J Mol Liq* 229:548–554. <https://doi.org/10.1016/j.molliq.2016.12.18>

17. Jeyaram S (2021) Study of third-order nonlinear optical properties of basic violet 3 dye in polar protic and aprotic solvents. *J Fluoresc*. <https://doi.org/10.1007/s10895-021-02796-z>
18. Sheik-Bahae M, Said AA, Wei T, Hagan DJ, Van Stryland EM (1990) Sensitive measurement of optical nonlinearities using a single beam. *IEEE J Quant Elect* 26:760–769. <https://doi.org/10.1109/3.53394>
19. Sheik-Bahae M, Said AA, Van Stryland EM (1989) High-sensitive single beam n_2 measurements. *Opt Lett* 14:955–957. <https://doi.org/10.1364/OL.14.000955>
20. Pramodini S, Poornesh P (2013) Thermally induced nonlinear optical response and optical limiting of acid blue 40. *Curr Appl Phys* 13:1175–1182. <https://doi.org/10.1016/j.cap.2013.03.002>
21. Meng Q, Yan W, Yu M, Huang D (2003) A study of third-order nonlinear optical properties for anthraquinone derivatives. *Dyes Pigm* 56:145–149. [https://doi.org/10.1016/S0143-7208\(02\)00123-7](https://doi.org/10.1016/S0143-7208(02)00123-7)
22. Jeyaram S, Geethakrishnan T (2017) Low power laser induced NLO properties and optical limiting of an anthraquinone dye using Z-scan technique. *J Mater Sci Mater Elect* 28:9820–9827. <https://doi.org/10.1007/s10854-017-6763-6>

Publisher's Note Springer Nature remains neutral with regard to jurisdictional claims in published maps and institutional affiliations.